Current Signature Analysis for Diagnostics in Motor Bars under Locked Rotor Condition

Michael Hrelrison F. da Silva and Pyramo P. da Costa Jr.
Department of Electrical Engineering, Pontifícia Universidade Católica de Minas Gerais, Belo Horizonte, Brazil
Email: michaelhfsilva@gmail.com; pyramo@pucminas.br

***Abstract*—Three-phase induction motors are widely used in industrial electric applications. To ensure their operability, efforts have been made mainly in the detection of rotor faults. This work aims to detect rotor faults in induction motors through of Motor Current Signature Analysis (MCSA) under locked rotor condition. In this configuration, the procedure is most suitable for drives where the motor operates intermittently, with a short operating stroke or variable speed. This paper proposes a methodology and presents a comparison of consolidated signal processing techniques such as fast Fourier transform (FFT), Discrete Wavelet Transform (DWT), and Discrete Hilbert Transform (DHT) applied on the conventional input currents and components of Park transformation in a case study. The objective is to define which of the techniques is the most robust in the process of identifying broken bars in the induction motor for the proposed methodology.**

***Index Terms*—Induction motor, fault diagnosis, MCSA, broken bar, locked rotor, wavelet, Hilbert transform, Park transformation**

I. Introduction

Three-phase induction motors are widely used in industrial systems due to their versatility, simplicity, and cost-effectiveness. In this context, studies on fault detection techniques of those devices have been expanded to ensure the operation of the industrial systems. One of the main fault detection techniques used is the Motor Current Signature Analysis (MCSA). This technique is based on the analysis of the frequency spectrum of the motor current, for the identification of rotor or stator faults, through the identification and evaluation of their fault component magnitude inside the spectrum, usually applying the fast Fourier transform (FFT) [1]. MCSA may still be accompanied by another detection technique, thereby increasing accuracy where the FFT does not provide sufficient information for diagnosis. Among those techniques are the discrete wavelet transform (DWT), which decomposes a signal into several times and frequency scales, and the discrete Hilbert transform (DHT), which reflects how much the current phase energy varies in time [2], [3]. The MCSA may further run on the direct component *d*, the quadrature component *q*, and zero component 0 of the Park transformation applied to input current [4]. Those techniques are consolidated, and they are often used for the identification of rotor faults in squirrel cage induction motor since direct testing is not possible on it.

Most of the applications of the MCSA techniques are associated with drives and induction motor at a constant speed and high slip where they can be applied on online mode, thus without stopping the production process [5]. A high slip allows a better distinction of the fault harmonic components in the current spectrum. However, in some applications, the slip is small, which requires a large measurement time window and a high-resolution test instrument. Even so, at some variable speed applications, it is not possible to use a large measurement time window due to the short operating stroke, which means, it is limited to a few revolutions of the rotor. In this condition, for the motor to rotate freely, it must be decoupled from the load and an offline technique for fault detection applied. In some even more specific drives, the stroke is short and there is no possibility, or it is unfeasible to decouple the load. This condition requires a specific methodology to detect motor failures and it is the subject of this paper.

The MCSA technique for those drives must be performed under locked rotor conditions. This is necessary to obtain a larger sample window of the motor current. This way, it also allows filtering mechanical harmonic components, eliminating their interferences which are more easily identified in mechanical tests such as vibration analysis [6]. Those interferences refer to bearings, ventilation or cooling, rotor structure, mechanical actuation, load variation, etc., failures related to mechanical rotation which do not suffer interference from the motor rotating field. Another advantage of carrying out the test in this way is that rotor speed measurement is not necessary for measurement of slip (information necessary for the identification of fault components in the spectrum), since the rotor is blocked the slip has the value of the applied voltage frequency. This configuration also allows an easier current and frequency monitoring. Thereby, if the motor is fed by an inverter, it is possible to choose the best current and frequency for the test. A low frequency applied can favor low-resolution test instruments and filter high-frequency interferences. A high current can improve signal amplitude itself.

Manuscript received December 18, 2020; revised February 20, 2021; accepted April 1, 2021.
Corresponding author: Michael Hrelrison F. da Silva (email: michaelhfsilva@gmail.com).

doi: 10.18178/ijeetc.10.5.362-368

The motivation of this work came up during the maintenance of mining machines (such as electric rope shovel), where there is a high occurrence of motor failures. Some of those operations occur with low slip, short operating stroke, and difficult drive decoupling. Therefore, the need for the study was mainly due to rotor problems. Such a study is important to avoid mistaken maintenance that can last weeks in some cases on those machines.

This paper proposes a methodology applying MCSA, under locked rotor condition in a case study. The techniques used are FFT, DWT, and DHT transforms applied on the conventional input current and components of the Park transformation. The objective is to define which of the techniques is the most robust in the process of identifying broken bars in the induction motor for the proposed methodology. This work intends to support engineers with maintenance and as a database for researchers.

II. Related Works

Increased accuracy in a diagnosis can be established directly by increasing the input current measurement window or indirectly, by using the combination of more than one diagnostic technique and signal processing to emphasize fault characteristics. Direct methods as in [7] and [8] used FFT of zero sequence current, active and reactive power spectrum for detection. Other methods used the combination of FFT with mathematical morphology [9], empirical decomposition, [10] and independent component analysis [11] to improve the diagnosis. In the works [12] and [13], the direct application of the wavelet transform in spectrogram was presented. In [14], [15] and [16] were presented fault detection tools in online mode via FFT.

In [17] the application of an offline method with the rotor at zero speed was presented, but it did not use the conventional three-phase current for fault detection. It used a pulsating field with phase variation created by an inverter. Differently, the work developed here proposes comparing classical techniques such as FFT, DWT, and DHT with the rotor at zero speed, but using the conventional input current. The zero speed is obtained indirectly by adjusting the inverter speed controller. The test is made with a load on the shaft allowing higher amplitude of the input current, thus improving the diagnosis. In addition, the analysis for failure detection through the components of the Park transformation is presented and compared.

III. Theoretical Background

When a bar in a rotor breaks, the currents in the adjacent ones are raised by an armature reaction. The breaking of a bar generates mechanical asymmetry and as a result, electric distortion, magnetic distortion, and consequently, thermal stress. If f_s is the stator electric frequency, the rotor electric frequency f_r in the same direction equals to $(1-s)f_s$, where s is the slip. The asymmetry causes an sf_s component contrary to stator and rotor fields. Additionally, the stator electric frequency becomes $f_r-sf_s=(1-2s)f_s$ indicating the armature reaction. This is the basis for the investigation of asymmetry in induction motors. Due to torque pulsation, a component $(1+2s)f_s$ is induced and then, $f_0=(1\pm2s)f_s$ are the higher amplitudes, representing the bars frequencies around the fundamental in the spectrum of the stator current. Those are the basis for fault detection of rotor bars and are known as "sidebands" [1].

A. FFT

For the frequency domain analysis, the FFT is the main Fourier transform execution algorithm. The FFT is an algorithm that implements the discrete Fourier transform (DFT) reducing the number of calculations. The DFT requires n^2 multiplications for a signal of n samples. The FFT algorithm reduces it to $(n/2)\log_2 n$. One of the commonly used formats of the DFT is given by

$$X\left(\frac{n}{NT}\right)=\sum_{k=0}^{N-1}x(kT)e^{-\frac{j2\pi nk}{N}} \quad (1)$$

where n=0, 1, ⋯, N–1, N is the number of samples, and T is the sampling time interval [1].

B. DWT

Fourier transform decomposes a signal into a set of complex sine waves. Similarly, the wavelet transform decomposes a signal into a set of amplified and staggered versions of a wavelet. This process produces wavelet coefficients that are a function of scale and position. Wavelets can be asymmetrical, irregular, or discontinuous, unlike sine waves. Since the wavelets can take different shapes, scales, and positions, it can intensify signals of different types, frequencies and those that may not occur continuously in the sample. The discrete form of the wavelet transform is given by

$$x[n]=\sum_k a_{j_0,k}\phi_{j_0,k}[n]+\sum_{j=j_0}^{J-1}\sum_k d_{j,k}\varphi_{j,k}[n] \quad (2)$$

where $\phi[n]$ is the scalar function, $\phi_{j_0,k}[n]=2^{j_0/2}\phi(2^{j_0}n-k)$ is the scalar function at scale $s=2^{j_0}$ shifted by k, $\varphi[n]$ is the mother wavelet, $\varphi_{j,k}[n]=2^{j/2}\varphi(2^j n-k)$ is the mother wavelet at scale $s=2^j$ shifted by k, $a_{j_0,k}$ is the approximation coefficient at scale $s=2^{j_0}$, $d_{j,k}$ is the detail coefficient at scale $s=2^{j_0}$, and $N=2^J$, where N is the number of $x[n]$ samples [12]. One way to obtain the coefficients of the equation is to pass the signal through a high-pass and low-pass filter numerous times, each time dividing the sample quantity by two. This way, it obtains high frequency resolution at low frequencies and high time resolution at high frequencies [2].

C. DHT

The Hilbert transform is a specific linear operator that from a real function $x(t)$ of a real variable, produces another one in HT($x(t)$), given by the convolution within

function $1/(\pi t)$. This returns a complex signal called analytic signal, where the real part is the original signal, and the imaginary is the Hilbert transform. In frequency, the imaginary part is the real part shifted 90 ° in phase. The Hilbert transform series has the same amplitude and frequency as the original signal, and it includes phase information that depends on the original phase. In addition, the analytic signal contains only positive frequencies in the frequency spectrum. One commonly used way to indirectly obtain the analytic signal of a discrete signal $X[m]$ is given by

1. Computing the DFT of $X[m]$;
2. Getting the positive spectrum by

$$Z[m]=\begin{cases} X[0],\ m=0 \\ 2X[m],\ 1\le m\le N/2-1 \\ X\left[N/2\right],\ m=N/2 \\ 0,\ N/2+1\le m\le N-1 \end{cases} \quad (3)$$

3. Computing an inverse DFT.

The DFT of a signal generates a spectrum with positive and negative frequencies (mirrored in the 0 axis). The removal of the negative spectrum results in the analytic signal spectrum. Thus, its inverse DFT obtains the analytic signal, where the real part is the original one and the imaginary is the Hilbert transform. With the DHT applied to the motor current, the fault frequency of rotor bars appears in $2sf_s$ in the Fourier transform of the analytical signal module [3].

IV. Methodology

The case study presented in this work uses three current samples, one per motor. The current samples have a time of 30 seconds approximately from phase *a*. The motors have the same characteristics and drive condition. Each one with its respective current sample refers to as *A*, *B*, and *C*. The induction motors are squirrel cage type, with 57 bars, 1500 HP, 6 poles, and 30Hz nominal.

The motors under study are applied in a drive with a short operating stroke, variable speed, coupled to the drive end and fed by an inverter. Then, for this specific application, the locked rotor condition is obtained indirectly through motor speed control, with a load suspended in the air and the inverter set to zero speed reference. In order to sustain the load in the air, the inverter applies the currents, as shown in Fig. 1 (a), to obtain the *A*, *B*, and *C* samples. It can be seen in this picture, the current applied by the inverter is around 200A in rms and 0.2Hz for the three motors. The motor slip has the same value of the frequency applied since the motor speed is zero (s=1). The load allows a higher amplitude of the input current, thus improving the diagnosis. It is also possible to observe the samples of 30 seconds, 4 to 6 current cycles.

For the current measurements, an i1010 AC/DC Fluke clamp meter was used. The oscilloscope used to acquire the data was a Dataq DI-530-USB with a sampling rate of 200kHz. Data extraction is processed in the oscilloscope software, the Windaq Waveform Browser. Even with a high sampling rate, the data extraction was intentionally limited to 3000 points of approximately 30 seconds of the entire record so that it was possible to test the algorithms in low resolution. The data are imported into MATLAB and FFT, DWT, DHT, and Park transformation are executed. Fig. 1 (b) illustrates the entire method applied.

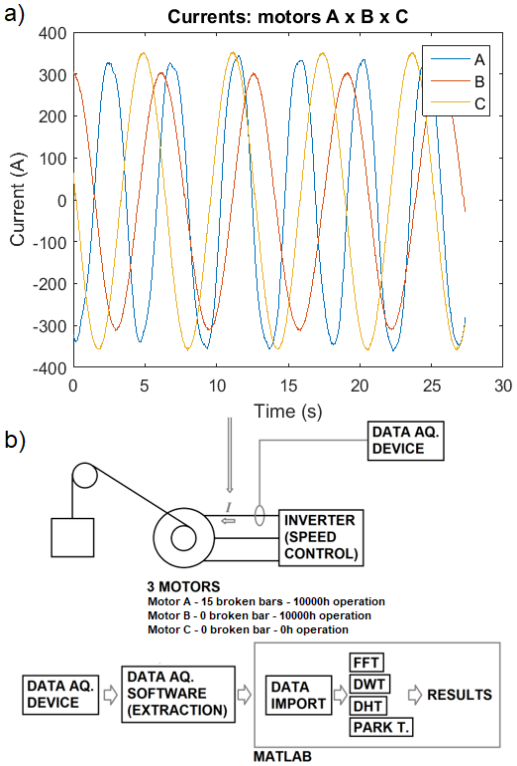

Fig. 1. Currents and methodology: (a) Currents samples of each test and (b) applied methodology.

V. Results

A. FFT

In Fig. 2 the FFT results of the three current samples are presented. The fundamental frequencies are observed in higher amplitude as indicated in the same color in Fig. 1. In *A*, a well-defined amplitude near to 0.7Hz is observed, which is the frequency component contained in the spectrum of the current, indicating broken rotor bars. The exact value is 0.693Hz, which corresponds to the fundamental plus two times the slip frequency (0.231+2×1×0.231). The frequencies of the bars in motors *B* and *C* are 0.456Hz and 0.480Hz, respectively, and as presented, there is no amplitude increased, indicating no failure. It is important to note that since the fundamental component is equal to the slip, there is not the smallest component of the sidebands, once this would be negative.

With the locked rotor, it has the exact value of the slip or bar frequency improving the resolution. The fault component is approximately 2 times higher compared with no-fault. It is known that the smaller the number of bars broken, the smaller the amplitude of its component within the frequency spectrum. Because of this, other methods can better evidence the condition of failure in a low number of broken bars.

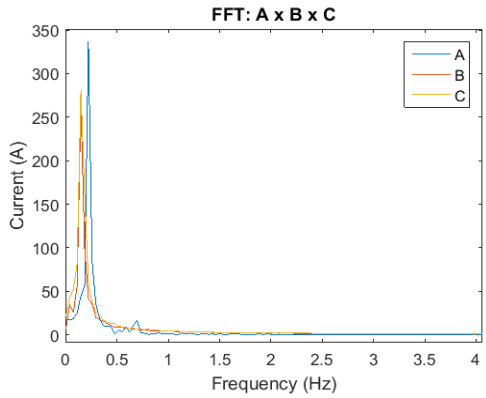

Fig. 2. FFT of *A*, *B*, and *C*.

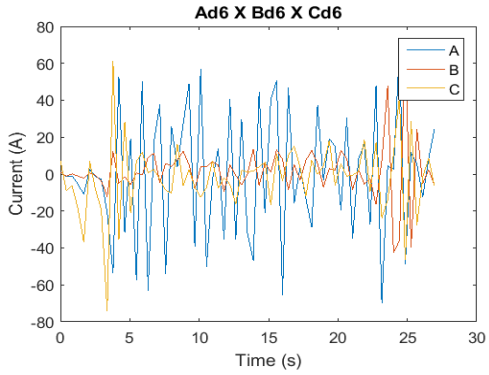

Fig. 3. Detail coefficient 6 from DWT of *A*, *B*, and *C*.

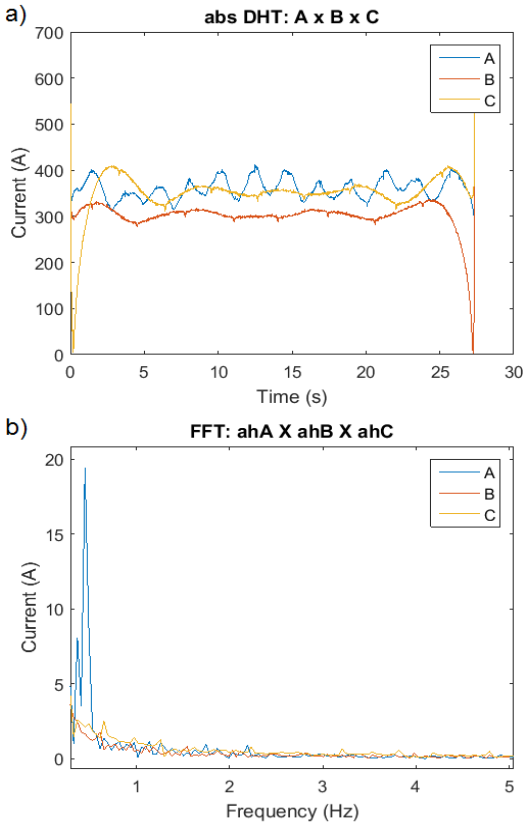

Fig. 4. Discrete Hilbert transform: (a) DHT currents modules and (b) their FFT of *A*, *B*, and *C*.

B. DWT

In Fig. 3, detail coefficient 6 of DWT via Daubechies 10 of the three motors current samples is presented. Detail coefficient 6 is the decomposition of the input signal (*A*, *B* and *C*) in high pass filter, with sample drop by two, executed six times. In detail 6 the fault component (fault frequency) is inside the frequency band this detail contains. It can be observed that the amplitude of this detail in *A* is superior to the healthy motors and that can be used as fault detection. The rms values indicate 34.2899A for the motor *A*, 15.1949A for the motor *B*, and 19.2467A for the motor *C*, 2 times higher approximately (outside the discontinuities it is 3 times).

Thus, it can be said that using the method via DWT simply analyzing rms value, a better fault definition is obtained compared to the one with FFT. However, it must consider the sample reduction, which in this case is reduced to approximately 65 points of the input signal with six decompositions. A low resolution may lead to false negative or positive detection.

C. DHT

Fig. 4 shows the results of the discrete Hilbert transform. As described in this paper, the DHT generates a complex signal and then, this transform will generate complex motor currents, the Hilbert currents. Fig. 4 (a) shows the module of those Hilbert currents obtained over the DHT of each current sample (*A*, *B*, and *C*). Their spectrum via FFT is in Fig. 4 (b). The failure detection with the Hilbert transform is based on the measurement of the amplitude of the fault component, which appears at frequency $2sf_s$, in the frequency spectrum obtained via FFT of the Hilbert current modules.

As can be seen in Fig. 4 (b), motor *A* has a difference in amplitude at frequency $2sf_s$ which offers great accuracy in the diagnosis of broken bars. 10 times higher amplitude is observed in fault conditions compared to no failure. Higher-resolution indicates even more clearly the spectrum failure characteristic.

D. Park Transformation, d and q

For the study presented, the measurement was not performed in the three phases of each motor, which is the ideal condition to perform Park transformation. To construct the three-phase current, a 120 ° shifting over *A*, *B* and *C* samples was performed to construct phases *b* and *c* (thus considering total symmetry in the motor and fault) and then Park transformation was applied. The FFT results of *d* and *q* currents from Park transformation are presented in Fig. 5 (a) and Fig. 5 (b).

As can be seen, there is only the fundamental component and the faulty one is attenuated in the spectrum. Some papers report good results using *d* and *q* currents to obtain fault characteristics [4]. However, in the configuration presented in this work, it does not demonstrate a good definition.

E. Park Transformation, 0

The Fig. 6 (a) shows 0 currents from Park transformation of motors *A*, *B*, and *C* with their respective FFTs in Fig. 6 (b). As all the other graphics in time domain in this paper, Fig. 6 (a) represents instantaneous values. As can be seen, all the asymmetry caused by broken bars is present in this component. It shows 20A in fault component of *A* while the faultless motors are close

to 0. Unlike the analysis in *d* and *q* currents, the method in this format presents robustness in fault detection.

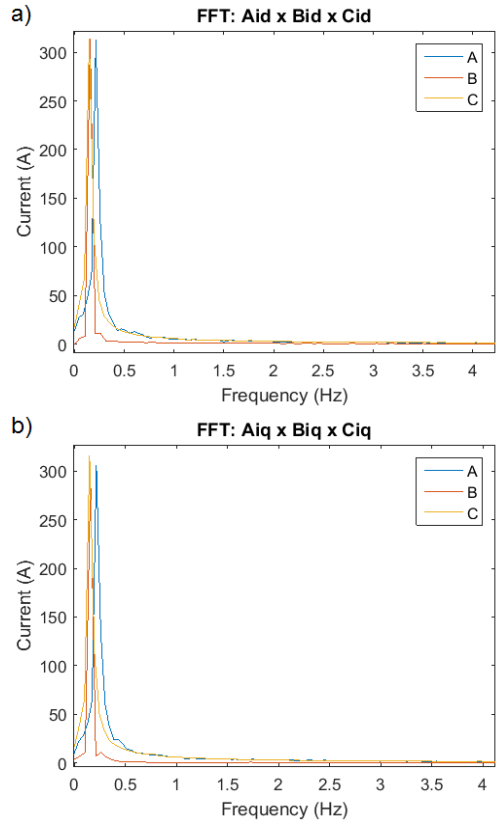

Fig. 5. Park transformation: (a) FFT of *d* and (b) *q* currents of Park transformation of *A*, *B*, and *C* motors.

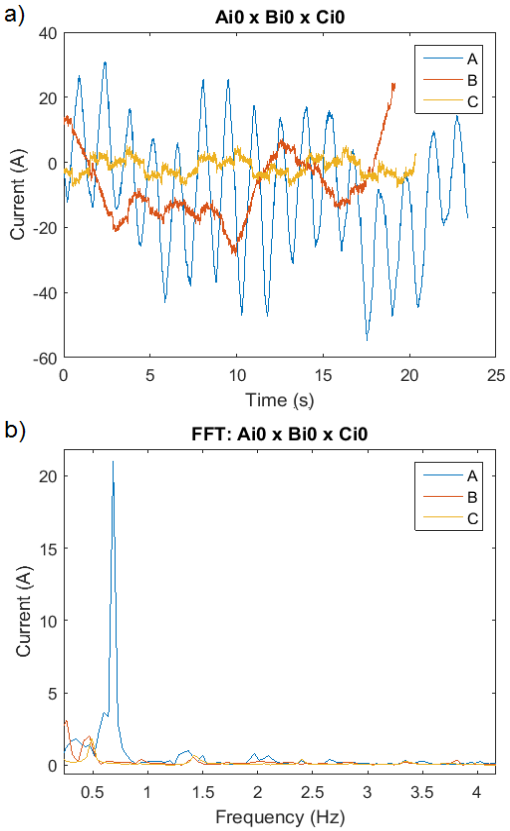

Fig. 6. Park transformation: (a) 0 currents of Park transformation and (b) their FFT of *A*, *B*, and *C* motor.

TABLE I: FAULT DEFINITION

Transform	*a*	*d*, *q*	0
FFT	2X	Undefined	>20X
DWT	3X	-	-
DHT	10X	-	-

VI. SUMMARY AND ANALYSIS

Table I shows the fault definition in this case study that summarizes the results with the tests performed with FFT, DFT and DHT using currents obtained from phase *a*, and FFT on the components of Park transformation. Each value approximately represents the ratio of the fault component magnitude to the faultless ones. It is important to notice that the results for FFT and DWT are obtained directly from their computation. For DHT, a FFT needs to be processed in order to have better fault definition. For the components of Park transformation, only FFT was applied.

The advantage of FFT is the availability in many field test instruments. If there is inaccuracy in the results, the other techniques presented can be used to improve diagnostic accuracy. In other tests outside the scope of this work, it was possible to verify the fault components with only 2 cycles of the input current in DWT, DHT or 0 current of the Park transformation and 3 cycles with FFT with a sample in higher resolution. This confirms that a higher sample rate and number of cycles covered by the transforms, a better resolution of the spectrum may increase the accuracy of the diagnosis. With the locked rotor, the exact value of the slip and the possibility of a large measurement time makes the application of the MCSA more accurate. The speed control with load on the shaft allows a higher amplitude in the input current, also improving the fault detection. It was possible to obtain fault definition with a few numbers of points due to the low frequency applied and it was not observed any interferences in the spectrums.

As presented, the motor rotor lockout was performed indirectly through speed control. Those tested motors are cooled by a blower and because of that, the tests could reach the 30 seconds of measurement. The locked rotor condition can also be obtained directly, thought mechanical locking of the rotor. In a loaded drive, the method studied here can be applied using the load itself as a block.

In the end, motor *A* was opened for inspection where 15 broken bars were identified of 57 it has. Fig. 7 is a picture of the rotor where it is possible to observe two totally and one partially broken.

Fig. 7. Broken bars in the motor *A*.

VII. Conclusion

The application of the MCSA method using FFT, DWT, DHT, and Park transformation demonstrated well defined fault indications in the presented drive system (short operating stroke, variable speed and coupled to the drive end) using the proposed methodology. A better fault indication was observed in DHT and 0 current of Park transformation, but direct FFT and DWT to the input current also presented good fault indications. For the application and number of broken bars present, currents *d* and *q* of Park transformation did not obtain results with failure indication.

The proposed methodology can be applied to any type of drive with an induction motor, as long as the system can remain at zero speed during the test.

There is no record of failure detection through 0 current of Park transformation as presented here and then, further tests can also be performed on future work for consolidation of the method.

Appendix A Park Transformation

Park transformation is a linear transformation that simplifies machine equations by introducing a set of hypothetical variables. Physically it transforms the machine with fixed stator windings and rotating rotor windings, into fixed stator windings and false-stationary rotor windings. Due to the sinusoidal variation of the mutual inductance, time-varying coefficients appears into the voltage equations. This effect can be eliminated by a change of variables which transform the stator and rotor voltages and currents into a common reference [4]. Fig. 8 shows the angular relationship between rotor and stator of a three-phase machine and an arbitrary axis *dq* rotating in an arbitrary speed. The transformation equations for the stator in a three-phase machine for axis *dq* at zero speed eliminating the mutual inductance variation are

$$f_{ds} = \frac{2}{3}\left[f_{as}\sin\theta + f_{bs}\sin\left(\theta - \frac{2\pi}{3}\right) + f_{cs}\sin\left(\theta + \frac{2\pi}{3}\right)\right]$$

$$f_{qs} = \frac{2}{3}\left[f_{as}\cos\theta + f_{bs}\cos\left(\theta - \frac{2\pi}{3}\right) + f_{cs}\cos\left(\theta + \frac{2\pi}{3}\right)\right]$$

$$f_{0s} = \frac{1}{3}\left(f_{as} + f_{bs} + f_{cs}\right)$$

where f can be represented by voltage, current or flux-linkage. For current, f_{as}, f_{bs} and f_{cs} are the stator current phases 1, 2 and 3 respectively. Thereby, f_{ds}, f_{qs} and f_{0s} are respectively the direct, quadrature, and zero component of the Park transformation applied to these stator currents.

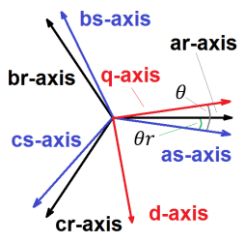

Fig. 8. Stator, rotor, and arbitrary axes relationship

Conflict of Interest

The authors declare no conflict of interest.

Author Contributions

Both authors contributed to the research, analysis, and development of this work. Michael Hrelrison F. da Silva was responsible for field collections, implementations, and algorithms on WWB and Matlab. Additionally, he performed the writing and formatting of this manuscript. Pyramo P. da Costa Jr. was responsible for guidance and review.

Acknowledgment

This study was financed in part by the Coordenação de Aperfeiçoamento de Pessoal de Nível Superior - Brasil (CAPES) - Finance Code 001. In addition, the authors wish to thank Pontifícia Universidade Católica de Minas Gerais as a base direct support and Sotreq S/A for the resources.

References

[1] J. Faiz, V. Ghorbanian, and G. Joksimovic, *Fault Diagnosis of Induction Motors*, 3rd ed. London, U.K.: Energy Engineering, Institution of Engineering and Technology, 2017, ch. 2, pp. 325-369.

[2] A. Bouzida, O. Touhami, R. Ibtiouen, A. Belouchrani, M. Fadel, and A. Rezzoug, "Fault diagnosis in industrial induction machines through discrete wavelet transform," *IEEE Trans. on Industrial Electronics*, vol. 58, no. 9, pp. 4385-4395, Sept. 2011.

[3] R. Puche-Panadero, M. Pineda-Sanchez, M. Riera-Guasp, J. Roger-Folch, E. Hurtado-Perez, and J. Perez-Cruz, "Improved resolution of the MCSA method via Hilbert transform, enabling the diagnosis of rotor asymmetries at very low slip," *IEEE Trans. on Energy Conversion*, vol. 24, no. 1, pp. 52-59, March 2009.

[4] J. Cusido, J. A. Rosero, J. A. Ortega, A. Garcia, and L. Romeral, "Induction motor fault detection by using wavelet decomposition on dq0 components," in *Proc. IEEE Int. Symposium on Industrial Electronics, Montreal*, 2006, pp. 2406-2411.

[5] S. B. Lee, D. Hyun, T. Kang, C. Yang, S. Shin, H. Kim, S. Park, T. Kong, and H. Kim, "Identification of false rotor fault indications produced by online MCSA for medium-voltage induction machines," *IEEE Trans. on Industry Applications*, vol. 52, no. 1, pp. 729-739, Jan.-Feb. 2016.

[6] E. Hashish, K. Miller, W. Finley, and S. Kreitzer, "Vibration diagnostic challenges: Case studies in electric motor applications," *IEEE Industry Applications Magazine*, vol. 23, no. 4, pp. 22-34, July-Aug. 2017.

[7] K. N. Gyftakis, J. A. Antonino-Daviu, R. Garcia-Hernandez, M. D. McCulloch, D. A. Howey, and A. J. M. Cardoso, "Comparative experimental investigation of broken bar fault detectability in induction motors," *IEEE Trans. on Industry Applications*, vol. 52, no. 2, pp. 1452-1459, March-April 2016.

[8] M. Drif, H. Kim, J. Kim, S. B. Lee, and A. J. M. Cardoso, "Active and reactive power spectra-based detection and separation of rotor faults and low-frequency load torque oscillations," *IEEE Trans. on Industry Applications*, vol. 53, no. 3, pp. 2702-2710, May-June 2017.

[9] J. D. J. Rangel-Magdaleno, H. Peregrina-Barreto, J. M. Ramirez-Cortes, P. Gomez-Gil, and R. Morales-Caporal, "FPGA-based broken bars detection on induction motors under different load using motor current signature analysis and mathematical morphology," *IEEE Trans. on Instrumentation and Measurement*, vol. 63, no. 5, pp. 1032-1040, May 2014.

[10] R. Valles-Novo, J. D. J. Rangel-Magdaleno, J. M. Ramirez-Cortes, H. Peregrina-Barreto, and R. Morales-Caporal, "Empirical mode

decomposition analysis for broken-bar detection on squirrel cage induction motors," *IEEE Trans. on Instrumentation and Measurement*, vol. 64, no. 5, pp. 1118-1128, May 2015.

[11] T. Yang, H. Pen, Z. Wang, and C. S. Chang, "Feature knowledge based fault detection of induction motors through the analysis of stator current data," *IEEE Trans. on Instrumentation and Measurement*, vol. 65, no. 3, pp. 549-558, March 2016.

[12] J. CusidÓCusido, L. Romeral, J. A. Ortega, J. A. Rosero, and A. Garc áGarcia Espinosa, "Fault detection in induction machines using power spectral density in wavelet decomposition," *IEEE Trans. on Industrial Electronics*, vol. 55, no. 2, pp. 633-643, Feb. 2008.

[13] Z. Ren, S. Zhou, C. E, M. Gong, B. Li, and B. Wen, "Crack fault diagnosis of rotor systems using wavelet transforms," *Computers Electrical Engineering*, vol. 45, pp. 33 – 41, July 2015.

[14] H. Guesmi, S. B. Salem, and K. Bacha, "Smart wireless sensor networks for online faults diagnosis in induction machine," *Computers Electrical Engineering*, vol. 41, pp. 226 – 239, January 2015.

[15] L. M. R. Baccarini, W. M. Caminhas, B. R. D. Menezes, H. N. Guimaraes, and L. H. Batista, "Sliding mode observer for rotor faults diagnosis," in *Proc. 32nd Annual Conf. on IEEE Industrial Electronics*, Paris, France, 2006, pp. 1345-1350.

[16] H. C. Chang, Y. M. Jheng, C. C. Kuo, and L. B. Huang, "On-line motor condition monitoring system for abnormality detection," *Computers Electrical Engineering*, vol. 51, pp. 255 – 269, April 2016.

[17] B. Kim, K. Lee, J. Yang, S. B. Lee, E. J. Wiedenbrug, and M. R. Shah, "Automated detection of rotor faults for inverter-fed induction machines under standstill conditions," *IEEE Trans. on Industry Applications*, vol. 47, no. 1, pp. 55-64, Jan.-Feb. 2011.

Michael Hrelrison F. da Silva was born in Belo Horizonte, Minas Gerais state, Brazil on 30th October 1982. He received B.Sc. degree in electrical engineering from the Centro Federal de Educação Tecnológica de Minas Gerais (CEFET-MG) in 2008 and his M.Sc. degree in electrical engineering with a specialization in motor fault detection from the Pontifícia Universidade Católica de Minas Gerais (PUC-MG) in 2019.

He is a currently technical consultant on electrical and automation systems of mining machines at Sotreq S.A, Brazil. With more than 25 years of experience in electrical systems and automation, his main function concentrates on the automation projects, electrical maintenance and failure analysis. His research interests are in modeling and application of current signature analysis techniques for failures in induction motors.

Pyramo P. da Costa Jr. received B.Sc. degree from Pontifícia Universidade Católica de Minas Gerais (PUC-MG) in 1970, M.Sc. degree from Universidade Federal de Minas Gerais (UFMG) in 1978 and Ph.D. degree from Universidade Estadual de Campinas (UNICAMP) in Electrical Engineering in 1982.

He is a currently professor at Pontifícia Universidade Católica de Minas. His experience in the area of Electrical Engineering, with emphasis on automation and control of electrical and industrial processes, working mainly on the following themes: neural networks, power transformer, fault diagnosis based on dissolved gas, computational intelligence on modeling and system identification, prediction of time series, evolutionary systems on construction of dynamic cluster in "datamining". He has contributed as a reviewer for the Journal Evolving Systems (Springer-Verlag) and Neural Computing and Applications.